

Diagnostic efficacy of gadoxetic acid-enhanced MRI for hepatocellular carcinoma and dysplastic nodule

Kazuhiro Saito, Fuminori Moriyasu, Katsutoshi Sugimoto, Ryota Nishio, Toru Saguchi, Toshitaka Nagao, Junichi Taira, Soichi Akata, Koichi Tokuyue

Kazuhiro Saito, Ryota Nishio, Toru Saguchi, Soichi Akata, Koichi Tokuyue, Department of Radiology, Tokyo Medical University, 160-0023 Tokyo, Japan

Fuminori Moriyasu, Katsutoshi Sugimoto, Junichi Taira, Department of Gastroenterology and Hepatology, Tokyo Medical University, 160-0023 Tokyo, Japan

Toshitaka Nagao, Department of Diagnostic Pathology, Tokyo Medical University, 160-0023 Tokyo, Japan

Author contributions: Saito K, Moriyasu F and Sugimoto K designed the research; Nishio R, Saguchi T, Nagao T and Taira J performed research; Saito K analyzed the data; and Saito K wrote the paper. Akata S and Tokuyue K gave final approval of the version to be published.

Correspondence to: Dr. Kazuhiro Saito, Department of Radiology, Tokyo Medical University, 160-0023 Tokyo, Japan. saito-k@tokyo-med.ac.jp

Telephone: +81-3-33426111 Fax: +81-3-33486314

Received: August 31, 2010 Revised: March 7, 2011

Accepted: March 14, 2011

Published online: August 14, 2011

Abstract

AIM: To evaluate the relationship between the signal intensity of hepatobiliary phase images on gadoxetic acid-enhanced magnetic resonance imaging (MRI) and histological grade.

METHODS: Fifty-nine patients with 82 hepatocellular lesions were evaluated retrospectively. Hepatobiliary phase images on gadoxetic acid-enhanced MRI were classified into 3 groups: low, iso or high. Angiography-assisted computed tomography (CT) findings were also classified into 3 groups: CT during arterial portography, and CT hepatic arteriography: A: iso, iso or low; B: slightly low, iso or low; and C: low, high. We correlated angiography-assisted CT, hepatobiliary phase findings during gadoxetic acid-enhanced MRI and histological grades. Furthermore, correlations between MRI findings and histological grade for each hemodynamic pattern were performed. Correlations among radiological

and pathological findings were statistically evaluated using the chi-square test and Fisher's exact test.

RESULTS: There was a significant correlation between histological grade and hemodynamic pattern ($P < 0.05$). There was a significant correlation between histological grade and signal intensity in the hepatobiliary phase ($P < 0.05$) in group A lesions. There was no significant correlation between histological grade and signal intensity in the hepatobiliary phase in group B or C lesions ($P > 0.05$).

CONCLUSION: Signal intensity in the hepatobiliary phase correlated with histological grade in the lesions that maintained portal blood flow, but did not correlate in lesions that showed decreased or defective portal blood flow.

© 2011 Baishideng. All rights reserved.

Key words: Hepatocellular carcinoma; Gd-EOB-DTPA; Gadoxetic acid; Primovist; Early hepatocellular carcinoma

Peer reviewer: Dr. Cuneyt Kayaalp, MD, Professor, Department of General Surgery, Staff Surgeon of Gastrointestinal Surgery, Turgut Ozal Medical Center, Inonu University, 44315 Malatya, Turkey

Saito K, Moriyasu F, Sugimoto K, Nishio R, Saguchi T, Nagao T, Taira J, Akata S, Tokuyue K. Diagnostic efficacy of gadoxetic acid-enhanced MRI for hepatocellular carcinoma and dysplastic nodule. *World J Gastroenterol* 2011; 17(30): 3503-3509 Available from: URL: <http://www.wjgnet.com/1007-9327/full/v17/i30/3503.htm> DOI: <http://dx.doi.org/10.3748/wjg.v17.i30.3503>

INTRODUCTION

Early detection of hepatocellular carcinoma (HCC) is im-

portant in establishing an effective therapeutic strategy^[1]. Early stage HCC does not have a hypervascular nature, and the lesions maintain portal blood flow^[2,3]. Intranodular portal blood flow can only be evaluated by computed tomography (CT) during arterial portography (CTAP), and the absence or decrease of portal blood flow in the nodule can show that the lesion is malignant^[4]. However, dysplastic nodules and some well-differentiated HCC lesions maintain portal blood flow, making differential diagnoses difficult^[5]. Gadolinium-ethoxybenzyl diethylenetriaminepentaacetic acid (gadoxetic acid, Primovist®; Bayer-Schering, Osaka, Japan) is a liver-specific contrast medium which is taken into hepatocytes and excreted into bile; therefore a T1 shortening effect in liver parenchyma is obtained. The hepatobiliary phase begins 1.5 min after injection of the contrast medium and continues for 2 h, and the peak liver signal intensity is obtained 20 min after injection of contrast medium^[6]. In the hepatobiliary phase, the tumor does not have normal functioning hepatocytes and is hypointense in most cases^[7]. However, several investigators reported that some HCC can be iso or hyperintense regardless of overt HCC^[8,9]. Gadoxetic acid-enhanced magnetic resonance imaging (MRI) yields a high tumor detection rate^[10] and can detect lesions that maintain portal blood flow using angiography-assisted CT^[11]. Therefore, gadoxetic acid-enhanced MRI can potentially distinguish the histological grade of hepatocellular lesions. We evaluated the relationships among angiography-assisted CT, hepatobiliary phase findings during gadoxetic acid-enhanced MRI and histological grades, and evaluated the diagnostic efficacy of gadoxetic acid for HCC and dysplastic nodule.

MATERIALS AND METHODS

Subjects

This retrospective study was approved by the Institutional Review Board, and the need for written informed consent was waived. Between January 2008 and June 2009, 460 patients received gadoxetic acid-enhanced MRI. Among them, patients satisfying all of the following criteria were enrolled; (1) **gadoxetic acid-enhanced MRI had been performed**; (2) **angiography-assisted CT had been performed**; (3) **the duration between gadoxetic acid-enhanced and angiography-assisted CT was less than 60 d**; and (4) **their lesions had been pathologically confirmed**. Patients in whom liver parenchymal enhancement was poor or absent due to severe portal hypertension or tumor invasion to the main portal vein were excluded. The subjects therefore consisted of 59 patients (37 men, 22 women), with 82 nodules. The mean age of the patients was 69 years (range 37-90 years). There were 8 patients with hepatitis B, 36 with hepatitis C, 4 alcoholic patients, 2 non-alcoholic patients with steatohepatitis, 1 with primary biliary cirrhosis and 8 cryptogenic patients. Six lesions were pathologically confirmed by operation. The other lesions were confirmed by ultrasound-guided biopsy (SSA-790A, Aplio XG; Toshiba Medical Systems Corp., Otawara, Japan). Biopsy specimens from the le-

sion and non-tumor area were obtained with a 20-gauge US-guided fine needle biopsy. Contrast medium (Sonazoid, Daiichi Sankyo, Tokyo, Japan) was used for obscure lesions on ultrasound. All lesions were detected on plain or contrast-enhanced ultrasound. The longest axis of the lesions was 5-66 mm (mean \pm SD, 17.4 mm \pm 9.5 mm). The longest dimension in 16 lesions was \leq 10 mm, 21 were \geq 10 mm, and 45 were $>$ 15 mm. The long axis was measured on MRI.

Imaging

Angiography-assisted CT was performed with an angiography-combined 16 detector row CT system (Advantx ACT, GE Medical Systems, Milwaukee, WI). Immediately after injecting prostaglandin E2 (Liple®; Mitsubishi Tanabe Pharma, Osaka, Japan) through a catheter, 76 mL of contrast material (Iomeprol 350 mgI/mL; Eisai, Tokyo, Japan), which was diluted twice with physiological saline, was injected at a rate of 2 mL/s. CTAP was obtained 30 s after beginning the injection of contrast material through a catheter in the superior mesenteric artery. The parameters for CT acquisition were: table speed, 13.7 mm/0.5 s; collimation, 10 mm; and reconstruction, 5 mm. CT hepatic arteriography (CTHA) was obtained 6 s after the injection of contrast material through a catheter in the common hepatic or proper hepatic artery. In cases of hepatic artery bifurcation variation, the catheter was first inserted into the right and then the left hepatic artery, or *vice versa*. A total of 10-30 mL of contrast material (Iomeprol 350 mgI/mL) was injected at a rate of 0.8-1.5 mL/s. CTHA was obtained in 3 phases. Immediately after finishing the first phase, the second phase was obtained, and the third phase was obtained 2 min after beginning the injection of contrast material.

MR images were obtained using a 1.5 T superconductive MRI system (Avanto; Siemens, Erlangen, Germany). T1 weighted images (T1WI) included in-phase and opposed-phase images. The T1WI parameters (in-phase and opposed-phase) were: TR/TE, 120/4.76, 2.38 ms; flip angle, 75°; 1 averaging; matrix, 256 \times 140; parallel acquisition technique (PAT) factor 2 with generalized autocalibration partially parallel acquisition (GRAPPA) algorithm; slice thickness, 6 mm; slice gap, 1.2 mm; and acquisition time, 13 s. The T2WI parameters were: TR/TE, 3600/99 ms; flip angle, 150°; echo train length, 29; matrix, 256 \times 75(%); slice thickness, 6 mm; 1 averaging; PAT factor 2 with GRAPPA algorithm; and acquisition time, 14 s. T2WI was performed while subjects held their breath. 2 or 3 mL/s of gadoxetic acid (0.025 μ mol/kg) was injected *via* the antecubital vein followed by 20 or 40 mL of physiological saline. The dynamic study included the arterial phase, portal phase, and 4 min after injecting the contrast material. A 3-dimensional (3-D) volumetric interpolated breath-hold examination (3D-VIBE) was used with the dynamic study. The 3D-VIBE parameters were: TR/TE, 4.28/1.78 ms; flip angle, 15°; matrix, 256 \times 85 (%); PAT factor, 2; slice thickness, 3 mm; and acquisition time, 20 s. The monitoring scan technique (Care Bolus method) was used to obtain the optimal arterial phase. The hepato-



Figure 1 A 69-year-old man with moderately differentiated hepatocellular carcinoma. A: Computed tomography (CT) hepatic arteriography shows hypodensity; B: CT during arterial portography shows isodensity; C: Lesion clearly shows hypointensity in the hepatobiliary phase during gadoxetic acid-enhanced magnetic resonance imaging (arrow).



Figure 2 A 72-year-old man with well differentiated hepatocellular carcinoma. A: Computed tomography (CT) hepatic arteriography shows faint hypodensity; B: CT during arterial portography shows faint hypodensity; C: The lesion clearly shows hypointensity in the hepatobiliary phase on gadoxetic acid-enhanced magnetic resonance imaging (arrow).

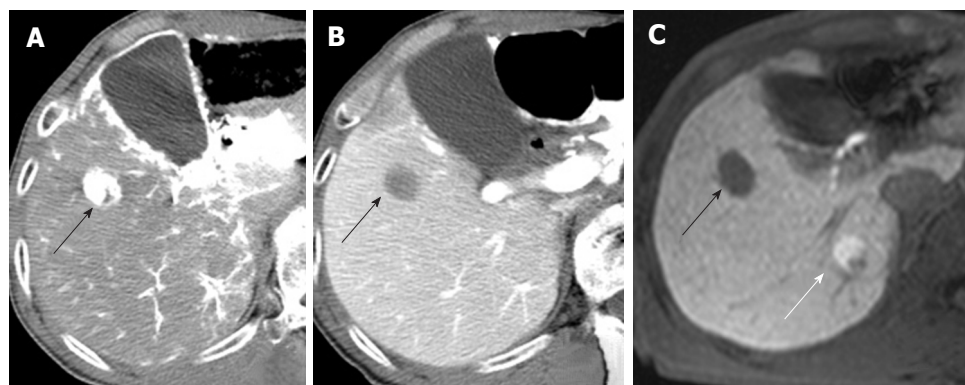


Figure 3 An 80-year-old man with poorly differentiated (black arrow) and well differentiated hepatocellular carcinoma (white arrow). A: Poorly differentiated hepatocellular carcinoma shows hypervascularity on computed tomography (CT) hepatic arteriography; B: Hypodensity on CT during arterial portography; C: Hypointensity in hepatobiliary phase on gadoxetic acid-enhanced magnetic resonance imaging (MRI). The lesion is not visible on CT hepatic arteriography (A) or on CT during arterial portography (B) and shows hyperintensity in the hepatobiliary phase on gadoxetic acid-enhanced MRI.

biliary phase was obtained with 3D-VIBE 20 min after injecting the contrast material.

Evaluation

A radiologist with 18 years of experience, whose specialty was interventional radiology, and a physician with 8 years of experience, whose specialty was liver imaging,

evaluated the angiography-assisted CT by consensus. The findings of angiography-assisted CT were classified into 3 groups based on a previous report^[12]: A, isodensity on CTAP and isodensity or low density on CTHA; B, slightly low density on CTAP and isodensity or low density on CTHA; and C, low density on CTAP and high density on CTHA (Figures 1-3). Partial hypodensity on CTAP and

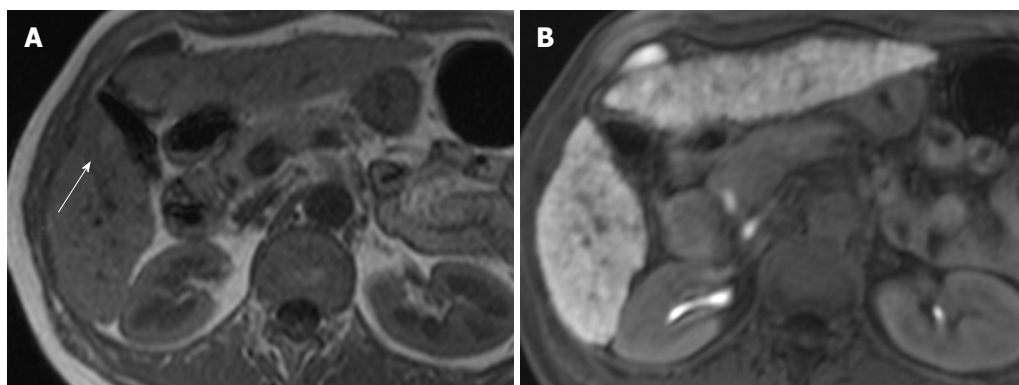


Figure 4 A 70-year-old woman with dysplastic nodule (arrow). A: The lesion shows hyperintensity on T1 weighted images; B: Isointensity in hepatobiliary phase on gadoxetic acid-enhanced magnetic resonance imaging.

Table 1 Correlation of histological grade and hemodynamic pattern

		Hemodynamic pattern			Total
		A	B	C	
Histological grade	DN	2	1	0	3
	Well	16 ²	8 ²	8 ¹	32
	Mod.	7 ¹	3	26 ²	36
	Poor	1	0	10 ²	11
Total		26	12	44	82

Hemodynamic patterns; A: Isodensity on computed tomography (CT) during arterial portography (CTAP) and isodensity or low density on CT hepatic arteriography (CTHA); B: Slightly low density on CTAP and isodensity or low density on CTHA; C: Low density on CTAP and high density on CTHA. DN: Dysplastic nodule; Well: Well differentiated hepatocellular carcinoma (HCC); Mod: Moderately differentiated HCC; Poor: Poorly differentiated HCC. ¹Significantly lower frequency; ²Significantly higher frequency.

partial high density on CTHA were included in group C.

Two radiologists with 18 and 8 years of experience respectively, whose specialty was abdominal diagnostic radiology, evaluated MRI by consensus. Lesion signal intensity in the hepatobiliary phase during gadoxetic acid-enhanced MRI compared with the surrounding liver parenchyma was classified as either hypointensity, isointensity, or hyperintensity (Figures 3, 4). The same evaluation was performed for T1WI and T2WI.

We correlated angiography-assisted CT, hepatobiliary phase findings during gadoxetic acid-enhanced MRI and histological grades. Furthermore, correlations between MRI findings and histological grade for each hemodynamic pattern were performed. The signal intensities of T1WI and T2WI also correlated with the signal intensities of the hepatobiliary phase.

Correlations among radiological and pathological findings were statistically evaluated using the chi-square test and Fisher's exact test. $P < 0.05$ was considered statistically significant. Statistical analysis was performed using SPSS version 16.0 (SPSS Inc., Chicago, IL, United States) for Windows.

RESULTS

Correlation of histological grade and hemodynamic pattern

Twenty-six, 12 and 44 lesions were classified into hemodynamic pattern types A, B and C, respectively. Type A included 2 dysplastic nodules, 16 well, 7 moderately and 1 poorly differentiated HCC. Type B included 1 dysplastic nodule, 8 well and 3 moderately differentiated HCC. Type C included 8 well, 26 moderately and 10 poorly differentiated HCC.

There was a significant correlation between histological grade and hemodynamic pattern ($P < 0.05$). Well-differentiated HCC showed hemodynamic patterns of types A and B with significantly high frequency, and that of type C with significantly less frequency. Moderately differentiated HCC showed the hemodynamic pattern of type A significantly less frequently, and that of type C with significantly high frequency. Poorly differentiated HCC showed the hemodynamic pattern of type C with significantly high frequency (Table 1).

Correlations between histological grade and signal intensity in the hepatobiliary phase

There was a significant correlation between histological grade and signal intensity in the hepatobiliary phase ($P < 0.05$). Dysplastic nodules showed isointensity with significantly high frequency and hypointensity with significantly less frequency. Moderately differentiated HCC showed significantly less isointensity frequency (Table 2).

Correlation between histological grade and signal intensity in the hepatobiliary phase in each hemodynamic pattern

Type A lesions: There was a significant correlation between histological grade and signal intensity in the hepatobiliary phase ($P < 0.05$). Dysplastic nodules showed isointensity with significantly high frequency and lower hypointensity (Table 3).

Type B and C lesions: There was no significant correlation between histological grade and signal intensity in the hepatobiliary phase in either hemodynamic pat-

Table 2 Correlation between histological grade and signal intensity in the hepatobiliary phase

		Hepatobiliary phase			Total
		Hyper.	Iso.	Hypo.	
Histological grade	DN	0	2 ²	1 ¹	3
	Well	1	3	28	32
	Mod.	1	0 ¹	35	36
	Poor	0	0	11	11
Total		2	5	75	82

DN: Dysplastic nodule; Well: Well differentiated hepatocellular carcinoma (HCC); Mod: Moderately differentiated HCC; Poor: Poorly differentiated HCC. Hyper: Hyperintensity; Iso: Isointensity; Hypo: Hypointensity. ¹Significantly lower frequency; ²Significantly higher frequency.

Table 3 Histological grade and signal intensity in the hepatobiliary phase in lesions which maintained portal blood flow

		Hepatobiliary phase			Total
		Hyperintensity	Isointensity	Hypointensity	
Histological grade	DN	0	2 ^b	0 ^a	2
	Well	1	0	15	16
	Mod.	0	0	7	7
	Poor	0	0	1	1
Total		1	2	23	26

DN: Dysplastic nodule; Well: Well differentiated hepatocellular carcinoma (HCC); Mod: Moderately differentiated HCC; Poor: Poorly differentiated HCC. ^aSignificantly lower frequency, $P < 0.05$; ^bSignificantly higher frequency, $P < 0.05$.

Table 4 Histological grade and signal intensity in the hepatobiliary phase in lesions with decreased portal blood flow

		Hepatobiliary phase		Total
		Isointensity	Hypointensity	
Histological grade	DN	0	1	1
	Well	1	7	8
	Mod.	0	3	3
	Poor	0	0	0
Total		1	11	12

DN: Dysplastic nodule; Well: Well differentiated hepatocellular carcinoma (HCC); Mod: Moderately differentiated HCC; Poor: Poorly differentiated HCC.

tern ($P > 0.05$) (Tables 4, 5).

Correlation between signal intensity on pre-contrast T1WI, T2WI and hepatobiliary phase

There was a significant correlation between the signal intensity of the T1-weighted in-phase image and that of the hepatobiliary phase ($P < 0.05$). The all isointense lesions in the hepatobiliary phase showed hyperintensity on T1-weighted in-phase imaging with significantly high frequency. The hyperintense lesions on T1-weighted in-phase imaging showed significantly less frequent hypointensity in the hepatobiliary phase. There were no significant correlations between the signal intensity of T1-weighted opposed-phase imaging and T2WI, or that of the hepatobiliary phase ($P > 0.05$) (Table 6).

Table 5 Histological grade and signal intensity in the hepatobiliary phase in lesions which lacked portal blood flow

		Hepatobiliary phase			Total
		Hyperintensity	Isointensity	Hypointensity	
Histological grade	DN	0	0	0	0
	Well	0	2	6	8
	Mod.	1	0	25	26
	Poor	0	0	10	10
Total		1	2	41	44

DN: Dysplastic nodule; Well: Well differentiated hepatocellular carcinoma (HCC); Mod: Moderately differentiated HCC; Poor: Poorly differentiated HCC.

Table 6 Correlation of signal intensity on pre-contrast T1WI, T2WI and hepatobiliary phase

		Hepatobiliary phase			Total
		Hyperintensity	Isointensity	Hypointensity	
T1WI	Hyperintensity	1	5 ^b	21 ^a	27
In-phase	Isointensity	0	0	27	27
	Hypointensity	1	0	27	28
T1WI	Hyperintensity	1	2	17	20
Opposed	Isointensity	0	3	23	26
phase	Hypointensity	1	0	35	36
T2WI	Hyperintensity	1	1	42	44
	Isointensity	0	4	27	31
	Hypointensity	1	0	6	7

^aSignificantly lower frequency, $P < 0.05$; ^bSignificantly higher frequency, $P < 0.05$.

DISCUSSION

According to previous angiography-assisted CT studies, it is still unclear whether lesions that maintain portal blood flow are dysplastic nodules^[13] or well-differentiated HCC^[5,14]. In the present study, the lesions that maintained portal blood flow included dysplastic nodules and various types of differentiated HCC. Furthermore, well-differentiated HCC had a significantly high rate of maintenance of portal blood flow. A similar result was previously reported^[14], indicating the presence of a high-grade malignant lesion within a small lesion that maintained portal blood flow.

Small HCC up to 1.5 cm in diameter and with an indistinct margin are called early HCC, and their malignant potential is relatively low^[2,3,15,16]. The lesions are characterized by a high prevalence of maintained portal blood flow, infrequent intrahepatic metastasis or portal invasion, and generally consist of well-differentiated HCC. This entity is hard to detect and distinguish from dysplastic nodules because of the similarity of radiological findings^[5,14,17,18], but it is clinically important to distinguish between these two entities. In the present study, isointense lesions in the hepatobiliary phase were dysplastic nodules or well differentiated HCC. Furthermore, among lesions maintaining portal blood flow, all isointense lesions were dysplastic nodules. However, hypointense lesions all appeared malignant. This finding may indicate that hypointense lesions, in which portal blood flow is maintained, are hepatocellular carcinoma.

Therefore, a combination of angiography-assisted CT and gadoteric acid-enhanced MRI should improve the accuracy of the diagnosis of hepatocellular lesions.

In the present study, signal intensity in the hepatobiliary phase significantly correlated with histological grade. Dysplastic nodules showed isointensity with significantly high frequency. However, some well differentiated HCC also showed isointensity. In the present study, some hypervascular well differentiated HCC showed isointensity while portal blood flow-maintained well differentiated HCC, with less malignant potential, showed hypointensity. In general, distinguishing between dysplastic nodules and well differentiated HCC in which portal blood flow is maintained is difficult. Dysplastic nodules appeared as hypo- or iso-vascular^[5,19,20]. Therefore the evaluation of tumor vascularity is important in distinguishing dysplastic nodules and hypervascular well differentiated HCC. The arterial phase is identifiable on gadoteric acid, and we consider that elucidating the optimal arterial phase for imaging is essential.

Some HCC showed hyperintensity in the hepatobiliary phase. This finding has been reported previously and appeared in well or moderately differentiated HCC^[8,11]. Narita *et al.*^[8] reported that uptake of gadoteric acid in HCC was determined by expression of the organic anion transporter 1B3 (OATP1B3). Therefore the degree of expression of OATP1B3 may influence signal intensity in HCC. This is partly because isointense lesions appeared in the hepatobiliary phase. Therefore, we speculated that one of the reasons why isointense lesions in the hepatobiliary phase appeared was due to the expression of OATP1B3, and the pathological appearance was extremely similar to the surrounding liver parenchyma.

All isointense lesions in the hepatobiliary phase were detected on MRI and showed hyperintensity in T1-weighted in-phase images in the present study. Pre-contrast MRI sequencing has been reported to be able to detect dysplastic nodules and well differentiated HCC^[21]. However, dysplastic nodules and well differentiated HCC frequently show hyperintensity^[22,23] on T1WI, and the present study emphasized the significance of T1-weighted in-phase images to detect these lesions.

The present study has several limitations. Most nodules were diagnosed by biopsy, and therefore, the classification of the histological grade of differentiation was judged using only the biopsied part of the lesions. Second, it is difficult to differentiate dysplastic nodules from early HCC using biopsy^[3] and there were few dysplastic nodules in the present study. Therefore further study is required.

In conclusion, signal intensity in the hepatobiliary phase on gadoteric acid-enhanced MRI was correlated with histological grade in the lesions that maintained portal blood flow, but did not correlate in the lesions with decreased or no portal blood flow. These findings suggest that lesions in which portal blood flow is maintained, and which appear hypointense in the hepatobiliary phase on gadoteric acid-enhanced MRI, are most likely to be HCC. These results indicate that gadoteric acid-enhanced MRI

can potentially be a powerful observation tool for HCC. These early-stage malignant lesions should be more easily detected, and enable appropriate work-up. This in turn should lead to improved clinical results of treatment.

ACKNOWLEDGMENTS

The authors are indebted to Mr. Roderick J Turner and Professor J Patrick Barron of the Department of International Communications of Tokyo Medical University for their review of the English manuscript.

COMMENTS

Background

Dysplastic nodules and some well differentiated hepatocellular carcinoma (HCC) lesions maintain portal blood flow, making differential diagnoses difficult. Gadoteric acid-enhanced magnetic resonance imaging (MRI) yields a high tumor detection rate and can detect lesions that maintain portal blood flow using angiography-assisted computed tomography (CT).

Research frontiers

According to previous angiography-assisted CT studies, it is still unclear whether lesions that maintain portal blood flow are dysplastic nodules or well differentiated HCC. In this study, the authors demonstrate relationships among angiography-assisted CT, hepatobiliary phase findings during gadoteric acid-enhanced MRI and histological grades.

Innovation and breakthrough

According to the present study, gadoteric acid-enhanced MRI should improve the accuracy of the diagnosis of hepatocellular lesions.

Applications

The lesions in which portal blood flow is maintained, and which appear hypointense in the hepatobiliary phase on gadoteric acid-enhanced MRI, have a greater probability of being HCC. Gadoteric acid-enhanced MRI can potentially be a powerful observation tool for HCC.

Terminology

Gadolinium-ethoxybenzyl diethylenetriaminepentaacetic acid (gadoteric acid) is a liver-specific contrast medium for magnetic resonance imaging which is taken into hepatocytes and excreted into bile, producing a T1-shortening effect in liver parenchyma. In the hepatobiliary phase, the tumor does not have normal functioning hepatocytes and is hypointense in most cases.

Peer review

This is a comparison with the pathological and radiological findings of dysplastic liver nodules and HCC. They found a close correlation with the histological grade and the intensity of the radiological views.

REFERENCES

- 1 **Takayama T**, Makuuchi M, Hirohashi S, Sakamoto M, Yamamoto J, Shimada K, Kosuge T, Okada S, Takayasu K, Yamasaki S. Early hepatocellular carcinoma as an entity with a high rate of surgical cure. *Hepatology* 1998; **28**: 1241-1246
- 2 **Honda H**, Tajima T, Taguchi K, Kuroiwa T, Yoshimitsu K, Irie H, Aibe H, Shinozaki K, Asayama Y, Shimada M, Masuda K. Recent developments in imaging diagnostics for HCC: CT arteriography and CT arteriportography evaluation of vascular changes in premalignant and malignant hepatic nodules. *J Hepatobiliary Pancreat Surg* 2000; **7**: 245-251
- 3 **Kojiro M**, Roskams T. Early hepatocellular carcinoma and dysplastic nodules. *Semin Liver Dis* 2005; **25**: 133-142
- 4 **Matsui O**, Kadoya M, Kameyama T, Yoshikawa J, Takashima T, Nakanuma Y, Unoura M, Kobayashi K, Izumi R, Ida M. Benign and malignant nodules in cirrhotic livers: distinction based on blood supply. *Radiology* 1991; **178**: 493-497
- 5 **Tajima T**, Honda H, Taguchi K, Asayama Y, Kuroiwa T, Yoshimitsu K, Irie H, Aibe H, Shimada M, Masuda K. Se-

- quential hemodynamic change in hepatocellular carcinoma and dysplastic nodules: CT angiography and pathologic correlation. *AJR Am J Roentgenol* 2002; **178**: 885-897
- 6 **Vogl TJ**, Kümmel S, Hammerstingl R, Schellenbeck M, Schumacher G, Balzer T, Schwarz W, Müller PK, Bechstein WO, Mack MG, Söllner O, Felix R. Liver tumors: comparison of MR imaging with Gd-EOB-DTPA and Gd-DTPA. *Radiology* 1996; **200**: 59-67
 - 7 **Reimer P**, Rummeny EJ, Shamsi K, Balzer T, Daldrup HE, Tombach B, Hesse T, Berns T, Peters PE. Phase II clinical evaluation of Gd-EOB-DTPA: dose, safety aspects, and pulse sequence. *Radiology* 1996; **199**: 177-183
 - 8 **Narita M**, Hatano E, Arizono S, Miyagawa-Hayashino A, Isoda H, Kitamura K, Taura K, Yasuchika K, Nitta T, Ikai I, Uemoto S. Expression of OATP1B3 determines uptake of Gd-EOB-DTPA in hepatocellular carcinoma. *J Gastroenterol* 2009; **44**: 793-798
 - 9 **Kim SH**, Kim SH, Lee J, Kim MJ, Jeon YH, Park Y, Choi D, Lee WJ, Lim HK. Gadoteric acid-enhanced MRI versus triple-phase MDCT for the preoperative detection of hepatocellular carcinoma. *AJR Am J Roentgenol* 2009; **192**: 1675-1681
 - 10 **Hammerstingl R**, Huppertz A, Breuer J, Balzer T, Blakeborough A, Carter R, Fusté LC, Heinz-Peer G, Judmaier W, Laniado M, Manfredi RM, Mathieu DG, Müller D, Mortelè K, Reimer P, Reiser MF, Robinson PJ, Shamsi K, Strotzer M, Taupitz M, Tombach B, Valeri G, van Beers BE, Vogl TJ. Diagnostic efficacy of gadoteric acid (Primovist)-enhanced MRI and spiral CT for a therapeutic strategy: comparison with intraoperative and histopathologic findings in focal liver lesions. *Eur Radiol* 2008; **18**: 457-467
 - 11 **Saito K**, Kotake F, Ito N, Ozuki T, Mikami R, Abe K, Shimazaki Y. Gd-EOB-DTPA enhanced MRI for hepatocellular carcinoma: quantitative evaluation of tumor enhancement in hepatobiliary phase. *Magn Reson Med Sci* 2005; **4**: 1-9
 - 12 **Shinmura R**, Matsui O, Kobayashi S, Terayama N, Sanada J, Ueda K, Gabata T, Kadoya M, Miyayama S. Cirrhotic nodules: association between MR imaging signal intensity and intranodular blood supply. *Radiology* 2005; **237**: 512-519
 - 13 **Hayashi M**, Matsui O, Ueda K, Kawamori Y, Kadoya M, Yoshikawa J, Gabata T, Takashima T, Nonomura A, Nakanuma Y. Correlation between the blood supply and grade of malignancy of hepatocellular nodules associated with liver cirrhosis: evaluation by CT during intraarterial injection of contrast medium. *AJR Am J Roentgenol* 1999; **172**: 969-976
 - 14 **Tanaka Y**, Sasaki Y, Katayama K, Hiramatsu N, Ito A, Murata H, Enomoto N, Oshita M, Mochizuki K, Tsujii M, Tsuji S, Kasahara A, Tomoda K, Nakamura H, Hayashi N, Hori M. Probability of hepatocellular carcinoma of small hepatocellular nodules undetectable by computed tomography during arterial portography. *Hepatology* 2000; **31**: 890-898
 - 15 **Kojiro M**, Nakashima O. Histopathologic evaluation of hepatocellular carcinoma with special reference to small early stage tumors. *Semin Liver Dis* 1999; **19**: 287-296
 - 16 **Kondo F**, Kondo Y, Nagato Y, Tomizawa M, Wada K. Interstitial tumour cell invasion in small hepatocellular carcinoma. Evaluation in microscopic and low magnification views. *J Gastroenterol Hepatol* 1994; **9**: 604-612
 - 17 **Li CS**, Chen RC, Tu HY, Shih LS, Zhang TA, Lii JM, Chen WT, Duh SJ, Chiang LC. Imaging well-differentiated hepatocellular carcinoma with dynamic triple-phase helical computed tomography. *Br J Radiol* 2006; **79**: 659-665
 - 18 **Muramatsu Y**, Nawano S, Takayasu K, Moriyama N, Yamada T, Yamasaki S, Hirohashi S. Early hepatocellular carcinoma: MR imaging. *Radiology* 1991; **181**: 209-213
 - 19 **Krinsky GA**, Lee VS, Theise ND, Weinreb JC, Rofsky NM, Diflo T, Teperman LW. Hepatocellular carcinoma and dysplastic nodules in patients with cirrhosis: prospective diagnosis with MR imaging and explantation correlation. *Radiology* 2001; **219**: 445-454
 - 20 **Lim JH**, Kim MJ, Park CK, Kang SS, Lee WJ, Lim HK. Dysplastic nodules in liver cirrhosis: detection with triple phase helical dynamic CT. *Br J Radiol* 2004; **77**: 911-916
 - 21 **Earls JP**, Theise ND, Weinreb JC, DeCorato DR, Krinsky GA, Rofsky NM, Mizrahi H, Teperman LW. Dysplastic nodules and hepatocellular carcinoma: thin-section MR imaging of explanted cirrhotic livers with pathologic correlation. *Radiology* 1996; **201**: 207-214
 - 22 **Li CS**, Chen RC, Lii JM, Chen WT, Shih LS, Zhang TA, Tu HY. Magnetic resonance imaging appearance of well-differentiated hepatocellular carcinoma. *J Comput Assist Tomogr* 2006; **30**: 597-603
 - 23 **Matsui O**, Kadoya M, Kameyama T, Yoshikawa J, Arai K, Gabata T, Takashima T, Nakanuma Y, Terada T, Ida M. Adenomatous hyperplastic nodules in the cirrhotic liver: differentiation from hepatocellular carcinoma with MR imaging. *Radiology* 1989; **173**: 123-126

S- Editor Sun H L- Editor O'Neill M E- Editor Zhang DN